Development of a Plate-Fin Type Gas Turbine Recuperator

Jae Su Kwak*

School of Aerospace and Mechanical Engineering, Hankook Aviation University,
200-1 Hwajeon-Dong Deogyang-Gu, Goyang-City, Gyeonggi-Do 412-791, Korea

Inyoung Yang

Aeropropulsion Department, Korea Aerospace Research Institute,
45 Eoeun-Dong, Yuseong-Gu, Daejeon 305-333, Korea

A plate-fin type recuperator for a gas turbine/fuel cell hybrid power generation system was designed, manufactured, and tested. Performance analysis shows that the performance of the system is directly affected by the performance of the recuperator. Therefore, the recuperator should be designed and manufactured carefully, and its performance should be tested and verified before it is integrated into the system. In this paper, the developing procedure including designing, manufacturing, and testing of a cross flow plate-fin type recuperator was presented. Performance test results showed that the design requirements of the recuperator were almost satisfied. Based on the test results, improved design to reduce the size of the recuperator was suggested.

Key Words : Heat Exchanger, Plate Fin, Gas Turbine Recuperator, Hybrid Power Generating System

Nomenclature

d	:	Throat diameter of venturi
D	:	Pipe diameter connected to venturi
$\dot{m}$	:	Mass flow rate (kg/s)
P_t	:	Total pressure (kPa)
Re	:	Reynolds number
T	:	Temperature (℃)
ΔP	:	Pressure difference of venturi
ΔP_t	:	Total pressure drop per stream
$\Delta P_{t,all}$	:	Overall total pressure drop

Greek

β	:	Diameter ratio of venturi (d/D)
η	:	Effectiveness of recuperator
ρ	:	Density of air at in-out averaged temperature

ρ_1	:	Density of air upstream venturi

Subscripts

c	:	Cold stream (air side)
h	:	Hot stream (exhaust gas side)
in	:	Recuperator inlet
out	:	Recuperator outlet

* Corresponding Author,
  E-mail : jskwak@hau.ac.kr
  TEL : +82-2-300-0103; **FAX** : +82-2-3158-4429
  School of Aerospace and Mechanical Engineering, Hankook Aviation University, 200-1 Hwajeon-Dong Deogyang-Gu, Goyang-City, Gyeonggi-Do 412-791, Korea. (Manuscript **Received** November 9, 2005; **Revised** April 4, 2006)
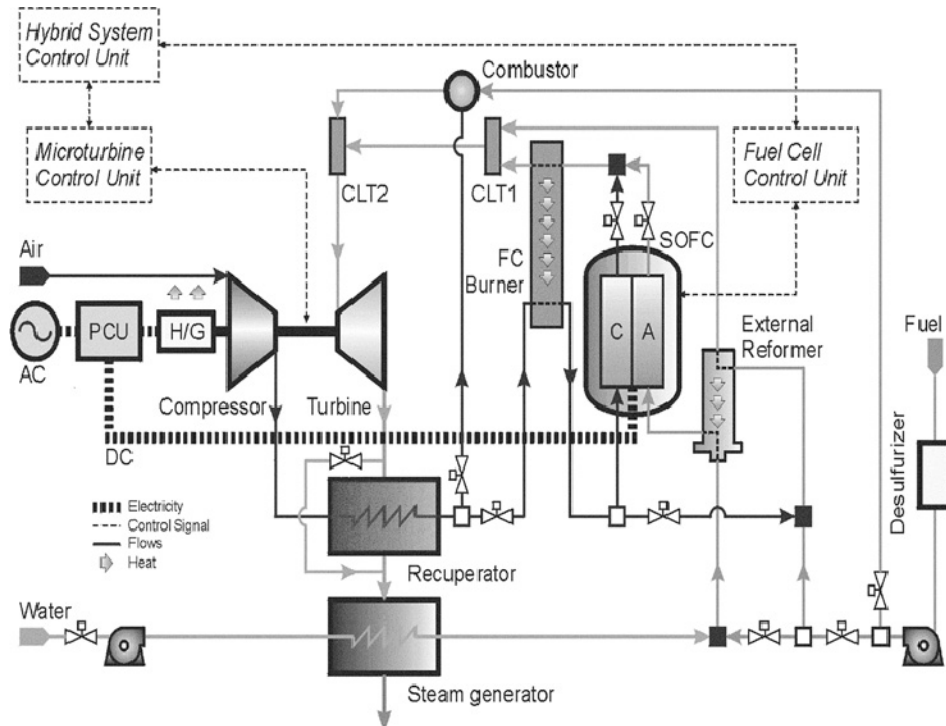
1. Introduction

In a gas turbine/fuel cell hybrid power generation system, the role of recuperator is to recover heat from gas turbine exhaust gas and to pre-heat compressed air which is supplied to the fuel cell system and the gas turbine combustor. System performance analysis shows that the system efficiency is very sensitive to the performance of the recuperator. One percent decrease of the recuperator effectiveness or one percent increase of the overall total pressure loss results in nearly one percent drop of the system efficiency. Thus, low pressure drop and high effectiveness are essential conditions of the recuperator. Figure 1 shows the schematic of the gas turbine/fuel cell power

Fig. 1 Schematic of gas turbine/fuel cell hybrid power generating system

generation system, which has been developed by KARI (Korea Aerospace Research Institute). The hot gas from the gas turbine combustor and the fuel cell are mixed and the mixed hot gas drives the turbine. Then, the turbine exhaust gas enters the recuperator and exchanges heat with the compressed air from the compressor, and proceeds to the steam generator. The compressed air from the compressor enters the recuperator and is preheated by the turbine exhaust gas, and sent to the fuel cell system and the gas turbine combustor. The effectiveness of the recuperator determines the temperature of the pre-heated compressed air and, as a result, determines the amount of fuel supplied to the gas turbine combustor and the fuel cell combustor. Accordingly, the effectiveness of the recuperator affects the system performance directly.

Plate-fin heat exchanger (PFHE) was selected as the recuperator in the project because of its compactness. Compared to other types of heat exchangers such as shell and tube type or plate type, PFHE has much higher surface area density (heat transfer area/volume). Therefore, the overall size of PFHE is much smaller than other heat exchangers with equivalent heat transfer capacity. Because the working fluids of the recuperator are filtered compressed air and burned gas of LNG, the fouling effect, which is one of the major obstacles to use PFHE, can be neglected in this case. The maximum operating temperature of a stainless steel PFHE can be as high as 800℃ and the maximum operating pressure of a stainless steel PFHE can be up to 16 bar at the operating temperature of 800℃ (Sumitomo Precision Product Co., 2006) Therefore, the required design condition of the recuperator, which will be presented later on, can be achieved by this type of heat exchanger.

Cross flow PFHE was selected as a recuperator in this project because it is easier to design and fabricate than the counter flow PFHE. A counter flow PFHE, which is more compact and efficient but more difficulty to design and manufacture, will be the next step of this development.

2. Design and Manufacture

Commercial PFHE designing software (Aspen Technology Inc., 2003) was used to design the core of the recuperator and another commercial software (Fluent Inc., 2004) was used to calculate the performance of headers.

Table 1 shows the design requirement of the recuperator. The effectiveness of the recuperator and the overall total pressure loss were defined by Eqs. (1) and (2), respectively. The overall total pressure drop includes the pressure drop of both streams.

$$\eta = \frac{T_{c,out} - T_{c,in}}{T_{h,in} - T_{c,in}} \qquad (1)$$

$$\Delta P_{t,all} = \frac{\Delta P_{t,c}}{P_{t,c,in}} + \frac{\Delta P_{t,h}}{P_{t,h,in}} \qquad (2)$$

Table 2 presents the operating conditions of the recuperator calculated by system performance analysis. The outlet condition of each stream was calculated based on the target effectiveness of 83% and the pressure drop of 3% for each stream.

The fin used in the design is plain type one. The height, thickness, and frequency of the fin are 5.10 mm, 0.203 mm, and 787 fins/m, respectively. Because the overall total pressure drop is one of the critical design factors of the recuperator, plain fin was used in the design in order to minimize the overall total pressure drop. Figure 2 presents the thermal and pressure drop characteristics of the fin. Fig. 2 shows that at the laminar region, i.e. Reynolds number is less than 2000, both Colborn factor and friction factor decreases as Reynolds number increases. In this work, because the range of Reynolds number at the fin is between about 80 and 170, it is expected that the effectiveness and pressure drop decrease as the Reynolds number increases in the range.

Table 3 shows the summary of the design results. The total number of layers is 132 and each side of stream has same number of layers. The fin plates were stacked in such a way that one stream layer is placed between the other stream layers. The thickness of the parting sheet was 1 mm, and the width and height of side bar were 12 mm and 5.1 mm, respectively

Table 1 Recuperator design conditions

Effectiveness	above 83%
Overall total pressure drop	below 6%
Maximum operating temperature	650℃
Maximum operating pressure	400 kPa
Type of recuperator	plain plate-fin type
Combustor fuel*	LNG

*combustor's fuel is LNG and combustion efficiency is 99.8%.
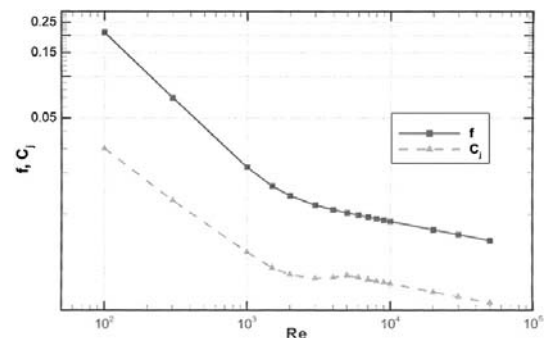
The calculated fraction of combusted gas is

$N_2 = 76.8\%$, $CO_2 = 1.2\%$, $O_2 = 18\%$, $H_2O = 4\%$

Table 2 Recuperator operating conditions

	Air side (cold stream)		Gas side (hot stream)	
	inlet	outlet	inlet	outlet
T (℃)	171	554.9	633.6	266.6
P_t (kPa)	349.32	338.84	107.67	104.44
Flow rate (kg/s)	0.67		0.6767	

Fig. 2 Thermal and pressure drop characteristic of the fin

Table 3 Design results of the recuperator

exchanger width (mm)	605.5
depth (stack height) (mm)	805.2
effective width (mm)	585.5
total number of layer	132
heat transfer area (m2)	442.32
side bar width (mm)	12
parting sheet thickness (mm)	1.0

Table 4 shows the estimated performance of the recuperator by the design software. In the performance calculation, fluid velocity and temperature were assumed to be uniform in all fins, and heat loss to the surrounding was neglected. The estimated effectiveness and the overall total pressure drop is 87.3% and 2.44%, respectively. Since the design margin of heat transfer area was 110% in the design, the estimated results showed better performance than the design conditions. In the performance estimation, the overall total pressure drop was calculated in the core only.

Because the design software can not design headers, separate designs and performance calculations were conducted for the headers (Hwang et al., 2004 ; Jeong et al., 2004). Figure 3 illustrates the cross section of the designed inlet header for both streams. Seven vanes and a baffle are placed in order to make core inlet flow as uniform as possible. Another role of the vanes was reinforcement of the header which operates at as high as 650°C. A baffle was installed just after the transition region from the circular pipe to the rectangular header. The thickness of the baffle was 5 mm and 10 mm-diameter holes were placed with a center-to-center distance of 12 mm. At the out-

let headers, vane or baffle was not used since the pressure drop in outlet header is much smaller than that in the inlet header. Table 5 shows the estimated performance of the cold side header (Hwang et al., 2004). The results show that the pressure drop at the inlet header is about seven times bigger than that at the outlet header.

Figure 4 describes the layout of the heat exchanger core. The core consists of 8 modules and each module has 16 or 18 fin layers. Individual

**Table 5** Estimated performance of the header (cold side)

ΔP_t at inlet header (kPa)	1.54
ΔP_t at outlet header (kPa)	0.21
ΔP_t (kPa)	1.75
Average V at core inlet (m/s)	4.41

Fig. 4 Layout of the heat exchanger core

Table 4 Calculated performance of the recuperator

	Air (cold stream)	Gas (hot stream)
T_{in} (°C)	171.0	633.6
T_{out} (°C)	574.92	256.13
$P_{t,in}$ (kPa)	349.3	107.7
ΔP_t (kPa)	−0.68	−2.42
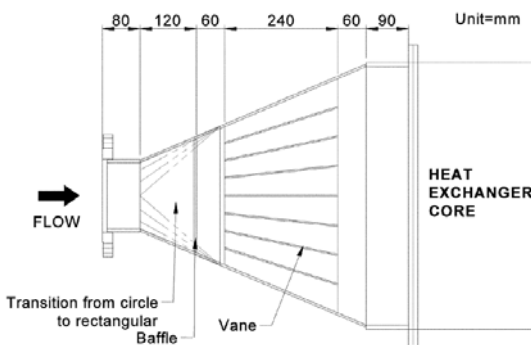
Fig. 3 Cross section of the inlet header
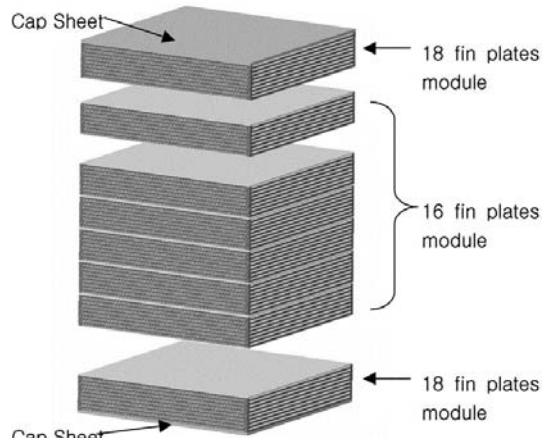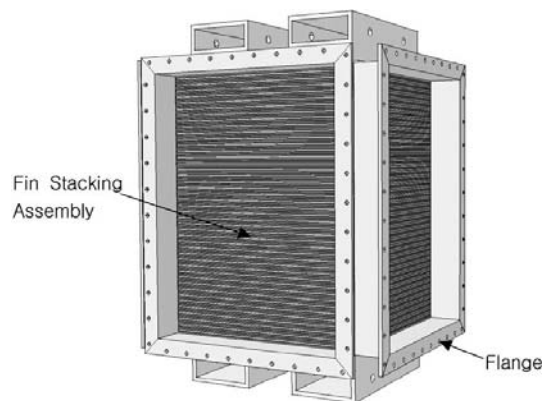
Fig. 5 Assembled core

modules were brazed separately, and then were welded together. STS316L was used for fins, parting sheets, side bars, cap sheets of the core and hot side headers. For the headers used in lower temperature condition (hot stream outlet and cold stream inlet), STS304 was used. After the core was assembled, flanges for the headers were welded on the core. Figure 5 illustrates the core assembled with flanges.

3. Test Facility

Performance tests of the manufactured recuperator were performed using air as working fluid for both hot and cold stream. Figure 6 illustrates the performance test facility installed at KARI. The test facility consists of an air compressor, two electric heaters with total power of 700 kW, flow meters for high temperature application, control valves to control flow rate and inlet pressure condition, combination probes to measure temperature and pressure at a time, and data acquisition system. The maximum mass flow rate and pressure of air supplied by the facility compressor is 2.1 kg/s and 4.2 bar, respectively. As shown in Fig. 6, a single compressor supplied air to both hot and cold stream of the recuperator. To heat each stream of air to the pre-determined test conditions, two heaters were used systemically. Bypassed unheated air and heated air were mixed and supplied to the cold side of the recuperator. For the hot stream, air was heated by both 300 kW and 400 kW heaters. Even though the pipe between the heaters and the recuperator was in-

sulated, heat loss to its environment was inevitable. To compensate for the heat loss, the supplied air was heated up to 710℃ which is above the required temperature at the recuperator's inlet (about 610℃). The flow rate of each stream was measured by a venturi flow meter made of STS 310. Total 4 control valves were installed upstream and downstream the recuperator to control mass flow rate and inlet pressure. Because air for both hot and cold streams was supplied from a single compressor, operation of a valve on one stream affected the mass flow rate and inlet pressure of the other stream. In the test, therefore, all of the four valves were controlled simultaneously in order to control the test condition.

At the inlet and outlet pipes connected to the headers, combination probes were installed to measure temperature, static pressure, and total pressure simultaneously. Combination probe is a Pitot tube, made of STS 310, with a thermocouple embedded inside and can be used in high temperature environment up to 920℃. At the inlet of each stream, temperature and pressure were measured just before air entered the header in order to take into account the pressure loss in the header. At the outlet of each stream, measurement was performed at just after air exits the outlet header. Because of the complex flow characteristic in the outlet header, the maximum temperature difference in the outlet measurement plane was over 150℃. To measure the mass-averaged temperature and pressure distribution at the outlet, 4 combination probes were installed with 45 degree
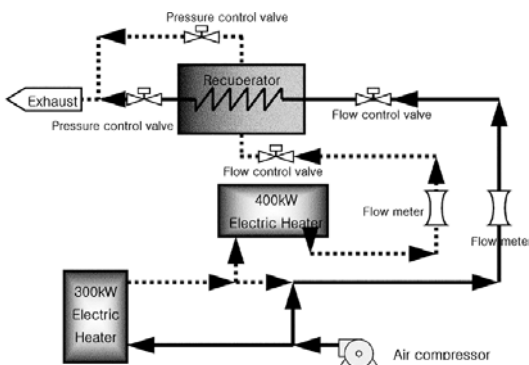

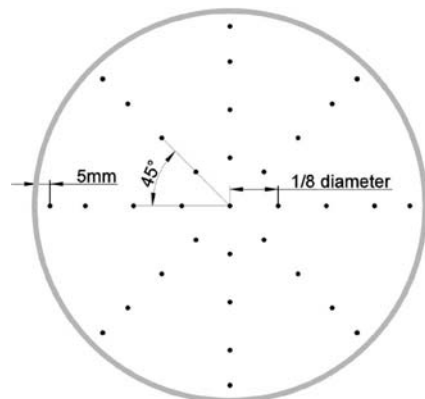**Fig. 6** Schematic of the performance test facility

Fig. 7 Measurement locations at outlet pipe

angle as shown in Fig. 7. Each combination probe was traversed and measured temperature and pressure at nine points. To avoid wall effect near the pipe wall, the minimum distance between the pipe wall and the tip of the combination probe was kept as 5 mm. The difference between the flow rate measured by the venturi flow meter and the mass-averaged flow rate by combination probes was less than 5%. At the inlet, because of long and straight inlet pipe, the distributions of temperature and velocity in the measurement plane were nearly uniform. Therefore, three K-type thermocouples and two combination probes were used to measure inlet conditions at the fixed locations.

Uncertainty assessment was performed for the key performance parameters, following ISO guide (International Organization for Standardization, 1995). For the mass flow rate measurement by venturi, Eq. (3) was used to calculate the air flow rate.

$$\dot{m} = C_d \frac{1}{\sqrt{1-\beta^4}} \frac{\pi}{4} d^2 \sqrt{2\Delta P \rho_1} \qquad (3)$$

All temperatures except cold stream outlet were time-averaged values of about 13,000 samples. $T_{c,out}$ was mass- and time-averaged. Table 6 shows the elementary measurement parameters, their nominal values and standard uncertainties. The calculated combined uncertainties of mass flow rate, effectiveness, were 0.0068 kg/s, 2.6%, respectively, and the standard uncertainty of the pressure was 241 Pa.

4. Performance Test Results

Performance tests were conducted for three different conditions. Table 7 shows test cases. Condition of case 1 was set to be close to the design condition. In case 2, hot side inlet temperature was about 40% lower than that of case 1, and mass flow rates of both streams for case 3 were about 45% less than those of case 1. In all cases, the mass flow rate of each stream was controlled to be similar to each other.

Figure 8 shows the temperature distribution at the cold stream outlet for case 1. As mentioned

Table 6 Measurement parameters and standard uncertainties

Performance Parameters	Elementary Measurement Parameters	Nominal value	Standard Uncertainty
$\dot{m}$	C_d	0.9885	1%
	d	82.75 mm	0.025 mm
	D	126.98 mm	0.025 mm
	ΔP	2274.0 Pa	33.90 Pa
	P_g	242.88 kPaG	1.980 kPa
	P_{amb}	101.20 kPaA	0.179 kPa
	T	446.45 K	1.118 K
$\Delta P_{T,all}$	$P_{T,h,in}$	112.93 kPaA	0.241 kPa
	$P_{T,h,out}$	109.14 kPaA	0.241 kPa
	$P_{T,c,in}$	346.36 kPaA	0.241 kPa
	$P_{T,c,out}$	345.38 kPaA	0.241 kPa
η	$T_{h,in}$	895.64 K	2.148 K
	$T_{c,in}$	443.80 K	2.148 K
	$T_{c,out}$	815.98 K	9.655 K
	$P_{T,c,out}$	345.38 kPaA	0.241 kPa
	$P_{S,c,out}$	344.90 kPaA	0.241 kPa

Table 7 Test cases

case	parameter	cold side	hot side	
1	$P_{t,in}$ (kPa)	346.36	109.14	reference case
	$\dot{m}$ (kg/s)	0.66	0.67	
2	$P_{t,in}$ (kPa)	341.18	110.78	lower $T_{h,in}$
	$\dot{m}$ (kg/s)	0.70	0.72	
3	$P_{t,in}$ (kPa)	342.03	104.61	lower $\dot{m}$
	$\dot{m}$ (kg/s)	0.36	0.36	
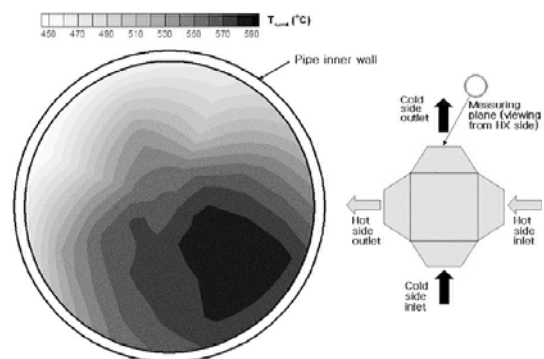
Fig. 8 Temperature distribution at cold side outlet (case 1)

previously, outlet temperature was measured by traversed combination probes. In Fig. 8, the temperature on the right side of measurement plane is higher than that on the left side of measurement plane. Because the hot stream entered from the right side, the temperature of air at the right side of the core is higher than that of the left side. That resulted in the distorted distribution of temperature at the outlet pipe. This result emphasizes that, at the heat exchanger outlet, measurement should be performed at as many as possible points and results should be mass-averaged.

Table 8 shows the test results and calculated results at each test condition. Because performance tests were conducted with air, the performance of the recuperator was calculated again with air as working fluid for both streams, as suggested by the American Society of Mechanical Engineer (2001). At near the design condition (case 1), the measured effectiveness and the overall total pressure drop was 82.4% and 3.64%, respectively. The measured effectiveness was 2.3% lower than the calculated one. The possible reasons for this deficiency in the effectiveness are flow mal-distribution and the heat loss to its surroundings. In the calculation, the velocity at the core inlet is assumed as uniform one, but is not uniform in the test case. Also, though 100 mm-thickness insulator was wrapped around the recuperator, some degree of heat loss is inevitable. Those two rea-

sons caused the difference in the measured and the calculated effectiveness. Test results also show that the pressure drop in hot stream is much higher than that in cold stream. This is caused by higher inlet velocity of the hot stream due to higher temperature (lower density).

The measured effectiveness of cases 2 and 3 were 4.7% and 8.2% lower than those by calculation, respectively, and those are much lower than case 1. The major possible cause of these differences is header design. The header was designed to be optimized at the design condition and the inlet flow may not be well-distributed at the off-design condition. Maldistribution of inlet air results in lower effectiveness. Ranganayakulu et al. (1997) calculated the effects of the inlet flow non-uniformity on the thermal performance and pressure drop in a cross flow compact PFHE. They showed that the effectiveness and the total pressure drop of a compact PFHE could be significantly affected by the non-uniformity of inlet flow. In some case, the deterioration in the effectiveness could be more than 20% compared to the uniform inlet flow case.

Figure 9 shows the effect of Reynolds number on the effectiveness. In this paper, the Reynolds number was defined as following:

$$\mathrm{Re} = \frac{\rho V D_h}{\mu} \qquad (4)$$

Table 8   Test and calculated results

	parameter	measured	calculated
Case 1	$\Delta P_{t,h}$ (kPa)	3.79	2.15 (core only)
	ΔP_{tc} (kPa)	0.28	0.64 (core only)
	$\Delta P_{t,all}$ (%)	3.64	2.16 (core only)
	η (%)	82.4	84.7
Case 2	$\Delta P_{t,h}$ (kPa)	2.79	1.55 (core only)
	ΔP_{tc} (kPa)	0.87	0.48 (core only)
	$\Delta P_{t,all}$ (%)	2.78	1.54 (core only)
	η (%)	80.8	85.5
Case 3	$\Delta P_{t,h}$ (kPa)	1.56	1.16 (core only)
	ΔP_{tc} (kPa)	0.48	0.35 (core only)
	$\Delta P_{t,all}$ (%)	1.63	1.21 (core only)
	η (%)	80.4	88.6
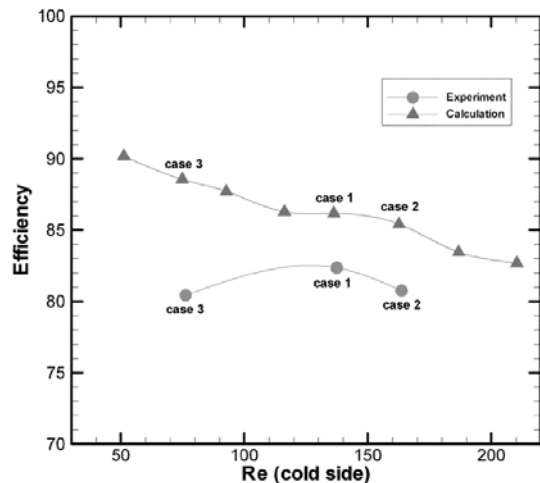
Fig. 9   Effect of Reynolds number on the effectiveness

In Eq. (4), D_h is the hydraulic diameter of the fin, V is the averaged velocity at the fin, and ρ and μ are density and viscosity of air at the averaged temperature of the inlet and the outlet of the stream. Since the mass flow rate and the in–out averaged temperatures of both streams were similar, the difference in calculated Reynolds number for both streams was less than 5%. In Fig. 9, Reynolds number calculated in the cold stream was presented. Figure 9 shows that the calculated effectiveness decreases as Reynolds number increases, which is due to the heat transfer characteristic of the fin. As Reynolds number increases, the Colburn factor of plain fin decreases as shown in Fig. 2, and results in decreased effectiveness. In the test results, the effectiveness of cases 1 and 2 show the trend, however, the effectiveness of case 3 is lower than the expected value. This is possibly caused by the flow mal–distribution. As mentioned previously, the header was designed to be optimized at the design condition and the flow distribution performance of the header can be worse in off–design conditions, especially at lower Reynolds number condition.

5. Improvement of design

In the test results of case 1, the effectiveness was a little bit lower than design requirement. However, the overall total pressure drop was about 40% lower than design condition. This means that there is a margin to reduce the cross sectional area of core, i.e. the total number of layer with given fin geometry and the size of fin plate. Figure 10 shows the effect of the number of layer on the effectiveness and the overall total pressure drop in the core. In Fig. 10, only the number of layer was changed, and fin height, width, and length were kept as constant. In the calculation, working fluids for hot and cold stream were gas turbine exhaust gas and compressed air, respectively. As the number of layer per stream increases from 35 to 55, the overall total pressure drop decrease by 37% (from 4.73 to 2.98%), while the effectiveness increases only 3.7% (83.2% to 86.2%). The overall total pressure drop is sensitive to the total number layer, while the sensitivity of the effec-
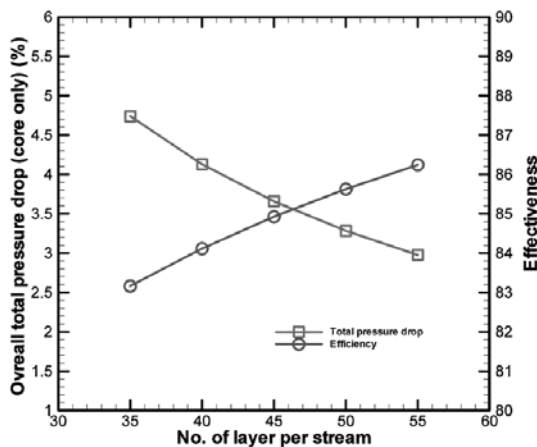

Fig. 10 Effect of the number of layer on the effectiveness and the overall total pressure drop

tiveness on the total number of layer is not significant. Figure 10 suggests that, if optimized headers are used and heat loss to its surroundings is minimized, the recuperator with less than 45 layers per stream could satisfy the design requirement of this work. This suggestion is based on the analysis by the design software only. However, because the comparison between the calculated and the test results showed that the accuracy of the design software was acceptable, it is expected that the suggestion would be valid with allowable error.

6. Conclusions

A cross flow plate–fin type recuperator for the gas turbine/fuel cell hybrid power generation system was designed, manufactured, and tested. In the design, commercial PFHE design software and commercial CFD software were used. Test results show that the measured performance of the recuperator almost satisfies its design condition. Also, test results show that, at the reference case, the measured effectiveness (82.4%) was lower than calculated one (84.7%), while the overall total pressure drop had about 40% margin. The analysis by the design software suggested that if the headers are optimized and the heat loss is minimized, the total number of layer can be reduced and, as a result, the manufacturing cost can

be also reduced.

References

Aspen Technology Inc., 2003, MUSE.

Fluent Inc., 2004, FLUENT.

Hwang, S. D., Cho, H. H., Kwak, J. S. and Yang, S. S., 2004, "A Numerical Analysis of Recuperator Header for Gas Turbine/Fuel Cell Hybrid Power Generating System," *Proceedings of The Third National Congress on Fluids Engineering*, pp. 899~902.

International Organization for Standardization, 1995, "Guide to the Expression of Uncertainty in Measurement," ISBN 92-67-10188-9, ISO.

Jeong, Y. J., Kim, S. Y., Kim, K. H., Kang, B. H., Kwak, J. S. and Yang, S. S., 2004, "Header Design of a Recuperator for a FC/GT Hybrid Power Generation System," *Proceeding of SAREK 2004 Summer Conference*, pp. 66~72.

Ranganayakulu, C. H., Seetharamu, K. N. and Sreevatsan, K. V., 1997, "The Effects of Inlet Fluid Flow Nonuniformity on Thermal Performance and Pressure Drops in Crossflow Plate-Fin Compact Heat Exchanger," *International Journal of Heat and Mass Transfer*, Vol. 40, pp. 27~38.

Sumitomo Precision Product Co. LTD, 2006, www.spp.co.jp

The American Society of Mechanical Engineer, 2001, "ASME PTC 12.5-200 : Single Phase Heat Exchangers," *ASME*, New York